BRAIN COMMUNICATIONS

Analysis of DNA from brain tissue on stereo-EEG electrodes reveals mosaic epilepsy-related variants

Alissa M. D'Gama,[1,2,3,*] H. Westley Phillips,[4,5,6,7,*] Yilan Wang,[6,7,8,*] Michelle Y. Chiu,[9,10] Yasmine Chahine,[7] Amanda C. Swanson,[11] Richard S. Smith,[12] Phillip L. Pearl,[9,10] Melissa Tsuboyama,[9,10] Joseph R. Madsen,[5] Hart Lidov,[13] Eunjung Alice Lee,[3,6,7] Sanjay P. Prabhu,[14] August Yue Huang,[3,6,7,†] Scellig S. D. Stone,[5,†] Christopher A. Walsh[3,6,7,8,10,15,†] and Annapurna Poduri[1,6,9,10,16,†]

* These authors contributed equally to this work.
† These authors contributed equally to this work.

Somatic mosaic variants contribute to focal epilepsy, with variants often present only in brain tissue and not in blood or other samples typically assayed for genetic testing. Thus, genetic analysis for mosaic variants in focal epilepsy has been limited to patients with drug-resistant epilepsy who undergo surgical resection and have resected brain tissue samples available. Stereo-EEG (sEEG) has become part of the evaluation for many patients with focal drug-resistant epilepsy, and sEEG electrodes provide a potential source of small amounts of brain-derived DNA. We aimed to identify, validate, and assess the distribution of deleterious mosaic variants in epilepsy-associated genes in DNA extracted from trace brain tissue on individual sEEG electrodes. We enrolled a prospective cohort of 10 paediatric patients with drug-resistant epilepsy who had sEEG electrodes implanted for invasive monitoring. We extracted unamplified DNA and in parallel performed whole-genome amplification from trace brain tissue on each sEEG electrode. We also extracted DNA from resected brain tissue and blood/saliva samples where available. We performed deep sequencing (panel and exome) and analysis for candidate germline and mosaic variants. We validated candidate mosaic variants and assessed the variant allele fraction in amplified and unamplified electrode–derived DNA and across electrodes. We extracted unamplified DNA and performed whole-genome amplification from >150 individual electrodes from 10 individuals. Immunohistochemistry confirmed the presence of neurons in the brain tissue on electrodes. Deep sequencing and analysis demonstrated similar depth of coverage between amplified and unamplified DNA samples but significantly more potential mosaic variants in amplified samples. We validated four deleterious mosaic variants in epilepsy-associated genes in electrode-derived DNA in three patients who underwent laser ablation and did not have resected brain tissue samples available. Three of the four variants were detected in both amplified and unamplified electrode–derived DNA, with higher variant allele fraction observed in DNA from electrodes in closest proximity to the electrical seizure focus in one case. We demonstrate that mosaic variants can be identified and validated from DNA extracted from trace brain tissue on individual sEEG electrodes in patients with drug-resistant focal epilepsy, from both unamplified and amplified electrode–derived DNA. Our findings support a relationship between the extent of regional genetic abnormality and electrophysiology and suggest that with further optimization, this minimally invasive diagnostic approach holds promise for advancing precision medicine for patients with drug-resistant epilepsy as part of the surgical evaluation.

1 Epilepsy Genetics Program, Department of Neurology, Boston Children's Hospital, Boston, MA 02115, USA
2 Division of Newborn Medicine, Department of Pediatrics, Boston Children's Hospital, Boston, MA 02115, USA
3 Department of Pediatrics, Harvard Medical School, Boston, MA 02115, USA
4 Department of Neurosurgery, Stanford University School of Medicine, Palo Alto, CA 94304, USA
5 Department of Neurosurgery, Boston Children's Hospital, Harvard Medical School, Boston, MA 02115, USA

Received October 01, 2024. Revised January 26, 2025. Accepted March 14, 2025. Advance access publication March 17, 2025
Published by Oxford University Press on behalf of the Guarantors of Brain 2025.

6 Broad Institute of MIT and Harvard, Cambridge, MA 02142, USA
7 Division of Genetics and Genomics, Manton Center for Orphan Disease Research, Boston Children's Hospital, Boston, MA 02115, USA
8 Program in Biological and Biomedical Sciences, Harvard Medical School, Boston, MA 02115, USA
9 Division of Epilepsy and Clinical Neurophysiology, Department of Neurology, Boston Children's Hospital, Boston, MA 02115, USA
10 Department of Neurology, Harvard Medical School, Boston, MA 02115, USA
11 Translational Neuroscience Center, Boston Children's Hospital, Boston, MA 02115, USA
12 Department of Pharmacology, Feinberg School of Medicine, Northwestern University, Chicago, IL 60611, USA
13 Division of Neuropathology, Department of Pathology, Boston Children's Hospital, Harvard Medical School, Boston, MA 02115, USA
14 Department of Radiology, Division of Neuroradiology, Boston Children's Hospital, Harvard Medical School, Boston, MA 02115, USA
15 Howard Hughes Medical Institute, Boston Children's Hospital, Boston, MA 02115, USA
16 National Institute of Neurological Disorders and Stroke, Bethesda, MD 20892, USA

Correspondence to: Annapurna Poduri, MD, MPH, National Institute of Neurological Disorders and Stroke
National Institutes of Health, 31 Center Drive, Bethesda, MD 20894, USA
E-mail: ann.poduri@nih.gov

Keywords: somatic mosaicism; drug-resistant epilepsy; epilepsy surgery; epilepsy genetics; stereo-EEG

Graphical Abstract

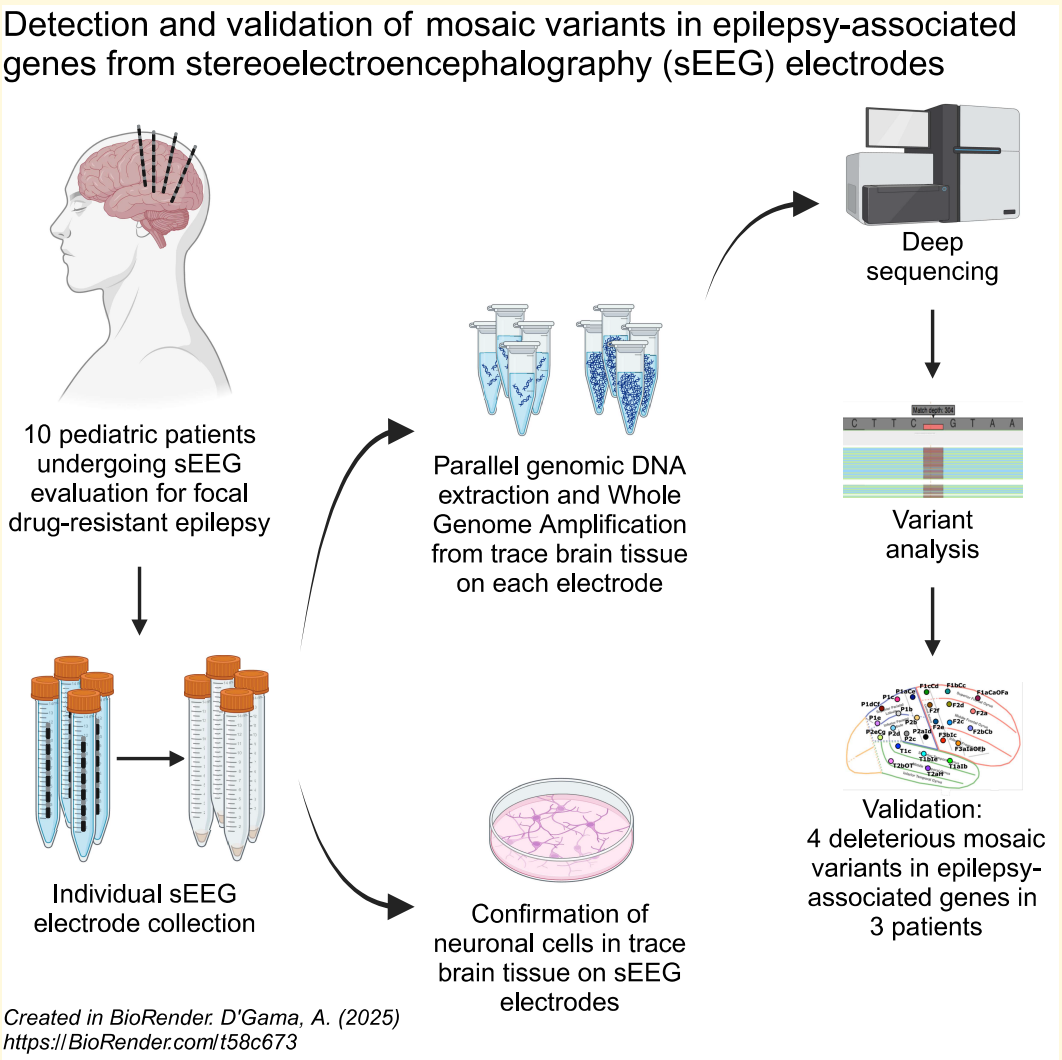

Introduction

Focal epilepsies, especially associated with malformations of cortical development (MCDs), are an important cause of paediatric drug-resistant epilepsy (DRE).[1] Initial treatment with anti-seizure medications (ASMs) remains largely empiric, and for individuals with focal DRE, surgical intervention provides a potential cure or palliative treatment.[2] The pathophysiologic basis for DRE encompasses many underlying aetiologies. Advances in massively parallel sequencing technologies over the past decade have accelerated progress in understanding the genetic aetiologies underlying many focal epilepsies and have demonstrated the important role of somatic mosaic variants, which arise from post-zygotic mutation, in MRI-lesional and, more recently, MRI-non-lesional focal epilepsies.[3-6]

Thus far, detection of mosaic variants in focal epilepsies has relied on access to surgically resected brain tissue samples, as many of these variants are brain limited and unable to be detected in clinically accessible tissues like blood or saliva.[7] Given the current workflow of brain tissue–based genomics, postoperative genetic diagnosis—following an open surgical procedure for DRE—is arguably 'too late' to guide precision medicine approaches and is not possible for patients who are ineligible for surgical resection or have minimally invasive interventions that do not involve brain tissue resection. Emerging diagnostic methods using alternative sources of brain-derived DNA, namely trace brain tissue from stereotactic EEG (sEEG) electrodes and cell-free DNA from CSF, provide an avenue for generating molecular genetic diagnosis prior to possible surgical resection and also in patients undergoing sEEG but not necessarily undergoing open cranial surgery.[8-13] sEEG involves the temporary implantation of multiple stereotactically directed depth electrodes into the brain to help localize a patient's seizure onset zone (SOZ). Following a period of typically several days of sEEG recording, the sEEG electrodes are explanted, at which point they have trace amounts of brain tissue attached to them. Six recent reports have demonstrated detection of mosaic variants in DNA extracted from trace brain tissue obtained from sEEG electrodes in a total of seven patients with focal epilepsy: one patient with peri-ventricular nodular heterotopia,[10] one patient with multi-focal non-lesional epilepsy,[9] three patients with focal cortical dysplasia (FCD),[12,14] one patient with a low-grade tumour[15] and one patient (from our group) with a diffuse frontal MCD.[16] Here, we report the results of deep sequencing DNA from explanted sEEG electrodes from a prospectively ascertained cohort, including 10 patients undergoing invasive intracranial monitoring for DRE. We detected and validated deleterious mosaic variants in epilepsy-associated genes in three patients who underwent sEEG and subsequently laser interstitial thermal therapy (LITT) rather than open surgical resection and who thus did not have resected brain tissue samples available. We demonstrate the feasibility of DNA recovery and mosaic variant detection from trace brain tissue from single sEEG electrodes in multiple patients with focal DRE and highlight aspects that require optimization for application of this minimally invasive diagnostic approach to broader groups of patients.

Materials and methods

Patient consent

We investigated 11 consecutive paediatric patients with DRE who had sEEG electrodes implanted as part of their epilepsy surgery evaluation at Boston Children's Hospital (BCH) and consented; one patient was previously reported,[16] and we report on the additional 10 patients here. Patients or their parents provided written informed consent to enrol in the BCH Rosamund Stone Zander Translational Neuroscience Center Human Neuron Core Repository for Neurological Disorders, which is offered to patients undergoing sEEG implantation and/or surgical resection for epilepsy at our institution. This study was approved by the BCH Institutional Review Board.

Sample collection and DNA extraction

sEEG electrodes were implanted intra-cranially using standard clinical techniques and labelled using the standardized electrode nomenclature for stereo-EEG applications (SENSAs).[17] Following several days of clinical monitoring for seizure and inter-ictal spike localization, sEEG electrodes were removed through their anchor bolts (hence limiting potential contact with extracerebral tissue), and each electrode was cut distal to the most superficial contact into a 15-ml conical tube containing 10 ml cold phosphate buffered saline (PBS). Tubes containing electrodes were transported on ice and either frozen at −80°C until processing or immediately processed. For processing, tubes were incubated for 4 h at 4°C, electrode tips were removed and tubes were centrifuged at 3500 rpm for 10 min at 4°C. The supernatant was removed, and the cell pellet was resuspended in 10 µl PBS + 4 mM $MgCl_2$. Three microlitres were used for whole-genome amplification of DNA using primary template-directed amplification (Bioskryb Genomics) per the manufacturer's protocol. The remaining 7 µl was used for extraction of unamplified DNA using the EZ1 DNA Tissue Kit (Qiagen) per the manufacturer's protocol. Where available, DNA from resected brain tissue samples was extracted using the EZ1 DNA Tissue Kit, and DNA from blood or saliva samples was extracted using Qiacube (Qiagen), per the manufacturer's protocols. DNA quantity and quality were assessed by TapeStation DNA ScreenTape analysis (Agilent).

Immunohistochemistry

Electrodes selected for immunohistochemical analysis were collected in the operating room into 15 ml conical tubes containing ice-cold Hibernate E media (ThermoFisher,

A1247601), a nutrient-rich media designed to preserve neural tissue, and transported on ice to the laboratory. Tubes containing electrodes were centrifuged at 500 rpm for 10 min followed by removal of 9.9 ml of the supernatant, with the remaining cell pellet resuspended in neuronal supporting tissue culture media (Neurobasal Plus + supplement media, ThermoFisher A3582901) with antibiotics penicillin/streptomycin (1%, ThermoFisher). Cells were plated onto tissue culture plates pre-treated with polyornithine and laminin to improve cell adherence. Cells were incubated at 37°C and 5% CO_2, with half media changes performed daily. On Day 2 post-electrode collection, adherent cells were fixed with 4% paraformaldehyde in PBS for 15 min at room temperature, washed and stored in PBS. Immunohistochemistry was performed as previously described.[18] Briefly, cells were blocked with goat serum and treated with triton 0.3%, and primary antibodies were incubated overnight against NeuN (MS-RBFOX3, EMD Millipore, MAB377) and microtubule-associated protein 2 (RB-MAP2, ThermoFisher, PA517646), followed with Alexa Flour secondary antibodies. Nuclear staining was performed with Hoechst 33342 stain. Epifluorescence images were captured using the Zeiss AxioObserver Epifluorescence microscope, and analysis was performed in ImageJ.

Deep panel and exome sequencing and analysis

Deep panel sequencing was performed on a subset of samples from the 10 patients; deep exome sequencing (ES) was additionally performed on a subset of samples from 8 patients (Supplementary Table 1). Panel sequencing was performed using a custom SureSelect XT HS2 panel (Agilent) that targeted the coding exons ±10 bp of 283 genes (target region of 852.4 kb). The panel included genes in the mammalian target of rapamycin (mTOR) pathway, which have been associated with disease-causing mosaic variants in lesional focal epilepsies,[19] genes in commercially available epilepsy gene panels, and genes in related cancer signalling pathways (Supplementary Table 2). ES was performed using a SureSelect XT HS2 Human All Exon V8 kit (Agilent). Libraries were prepared per the manufacturer's protocols and 2 × 150 bp paired-end sequencing was performed on Illumina HiSeq X (panel) or Illumina NovaSeq 6000 (ES) sequencers at Psomagen.

For the panel sequencing analysis, variant calling was performed using multiple methods. First, germline and mosaic variant calling was performed using SureCall (Agilent), which uses Burrows-Wheeler Alignment (BWA) for alignment to the reference human genome (hg19) and a proprietary variant caller (SNPPET) for variant calling. To achieve better sensitivity for mosaic variant detection, we further developed a customized pipeline to call mosaic single nucleotide variants (SNVs) and small insertions and deletions (indels) by MosaicHunter (version 0.1.4)[20] and Pisces (version 5.3),[21] respectively. For each sample, the raw fastq reads of each sample were trimmed with the AGeNT (version 2.0.5) Trimmer function before aligning to the reference genome (hg19) by BWA-MEM (version 0.7.15).[22] The PCR duplicates were then removed with the AGeNT (version 2.0.5) LocatIT function and local indels were realigned with GATK.[23] For mosaic variants detected by MosaicHunter and Pisces in each patient [variant allele fraction (VAF) 1–30%, supported by more than three reads], we performed sample-based filtering to remove potential germline contamination: all calls that appeared in blood samples were removed from the electrode samples and resected brain tissue samples; all recurrent variants among the blood samples were also removed.

For the ES analysis, raw fastq reads of each sample were aligned with BWA-MEM (version 0.7.15)[22] to the reference genome (hg19). The resulting bam files underwent preprocessing (mark duplicates, indel realignment and base quality recalibration) with Picard (version 1.138)[24] and GATK (versions 3.8 and 4.1.9).[23] Sequencing depth and the evenness of sequencing were visualized using customized Python scripts and BEDTools.[25] MosaicHunter was used to call mosaic SNVs with the recommended ES configurations.[20] We only considered mosaic calls with VAF <30% and excluded any calls present in dbSNP (version 138) or within 5 bp of germline indels in the same patient detected by GATK HaplotypeCaller (version 3.6).[23] To ensure a fair statistical comparison of the number of mosaic SNVs per sample, we sub-sampled the unamplified samples to the same mean depth as the amplified samples using Picard before re-running MosaicHunter and applying the same filtering procedures as described above. Variant discovery and validation were conducted on the variant call set without any subsampling.

Filtered variant calls were analysed for deleterious variants in genes associated with human disease that matched the patient phenotype. To reduce the likelihood of false positives, we required candidate mosaic variants to be present in more than one electrode sample for panel analysis as DNA from more than one electrode sample for each patient was included on the panel (versus DNA from only one electrode sample per patient was included for ES and thus available for ES analysis). Candidate mosaic variants were manually inspected using the Integrative Genomics Viewer (IGV)[26] prior to validation.

Amplicon sequencing validation

Candidate variants were validated using amplicon sequencing. Validation for each candidate variant was performed for multiple samples with remaining DNA from the relevant case. Custom primers were designed for each candidate variant using Primer3 (Supplementary Table 3), PCR amplification was performed using Phusion Hot Start II High-Fidelity DNA Polymerase (ThermoFisher), purification was performed using AMPure XP (Agencourt), and amplicons were sequenced on Illumina platforms using Amplicon-EZ (Genewiz). Raw fastq reads were aligned to the reference genome (hg19) using BWA-MEM (version 0.7.15)[22] and then processed for indel realignment using GATK (version 3.6).[23] To consider a variant as validated, we required the alternate allele of interest to have greater than three times the

number of reads as the other two alternate alleles. All validated variants were further manually inspected using IGV.[26]

Statistical analysis

We conducted pairwise comparisons for sequencing evenness (i.e. the percentage of coverage at ≥500×) of amplified sEEG electrode-derived DNA samples versus unamplified samples from resected brain tissue, blood/saliva and a few electrode samples in ES; sequencing depth of amplified versus unamplified samples in panel sequencing; sequencing depth of amplified versus unamplified samples in ES; number of mosaic SNVs in amplified versus unamplified samples in panel sequencing; number of mosaic indels in amplified versus unamplified samples in panel sequencing and number of mosaic SNVs in amplified versus unamplified samples in ES. To determine the appropriate statistical test, for each pairwise comparison, we first tested whether they were normally distributed using the Shapiro test. We next tested the equality of variances of the pair (homoscedasticity). If both were normally distributed (Shapiro test P-value ≥ 0.05), we used the Bartlett test; if at least one was not normally distributed (Shapiro test P-value < 0.05), we used the Levene test. Last, we tested the equality of mean based on the previous tests of normality and homoscedasticity. If the pair passed both tests (Bartlett test P-value ≥ 0.05), we used Student's t-test; if the pair failed either test (Shapiro test P-value < 0.05 or Bartlett test P-value < 0.05 or Levene test P-value < 0.05), we used the two-sided Mann–Whitney–Wilcoxon test. In both scenarios, the pair was determined to be significantly different if P-value is <0.05. All statistical tests were implemented using the Python SciPy library.[27]

Results

Recovery and sequencing of DNA from trace brain tissue on stereo-EEG electrodes

Ten consecutive paediatric patients with DRE who underwent sEEG electrode implantation as part of epilepsy surgery evaluation at BCH and consented to participating in research were included in this study (Table 1; Fig. 1A); an 11th patient was previously reported.[16] sEEG electrode tips were collected at the time of explantation, resected brain tissue samples were obtained for research sequencing when open resection was performed, and blood/saliva samples were obtained when possible. Immunohistochemistry confirmed the presence of neuronal (MAP2+) as well as non-neuronal (MAP2−) cells adherent to the explanted sEEG electrodes (Fig. 1B). We extracted unamplified DNA and performed whole-genome amplification of DNA from the brain tissue adherent to each of >150 electrodes, with higher concentration obtained from whole-genome amplified DNA (usually >50 ng/μl) compared with unamplified DNA (usually <10 ng/μl) (Supplementary Fig. 1). We thus primarily used amplified DNA samples for deep sequencing but included both amplified and unamplified DNA samples for validation.

We performed deep panel sequencing using multiple samples from each patient, including at least one sample from an electrode implanted into the presumed seizure onset focus from each patient, as well as resected brain tissue and blood samples when available (Supplementary Table 1). The panel focused on genes known to be associated with epilepsy, MCDs, and related cancer signalling pathways. Thus, for cases without confirmed MCDs like FCD, hemimegalencephaly (HME), or tuberous sclerosis complex (TSC) that are known to be associated with mosaic variants in genes included on the panel, we also performed deep ES to broadly evaluate all coding genes. For ES, we used a sample from an electrode implanted into the presumed seizure onset focus from each patient as well as resected brain tissue samples when available (Supplementary Table 1). Overall, the average depth of panel sequencing was 308× and of ES was 972×. For the ES samples, 63–96% of the targeted bases were sequenced to at least 500×, with the exception of the amplified sample from Patient 10, meaning that we could capture mosaic variants as low as VAF = 0.2% in these regions (Fig. 2A). For ES, the unamplified samples were sequenced more evenly than the amplified samples ($P = 0.049$, two-sided Mann–Whitney–Wilcoxon test with Bonferroni correction). Although sequencing depth did not significantly differ between amplified sEEG electrode-derived DNA samples versus unamplified samples from resected brain tissue, blood/saliva, and a few electrodes (two-sided Mann–Whitney–Wilcoxon test with Bonferroni correction, for panel sequencing, $P = 0.76$ and for ES, $P = 0.70$) (Fig. 2B and C), amplified samples had a significantly higher number of called mosaic SNVs and indels compared with unamplified samples (for panel sequencing, SNV $P = 4.5 \times 10^{-16}$, indel $P = 1.1 \times 10^{-16}$ and for ES, SNV $P = 0.049$, after sub-sampling the unamplified samples to the mean sequencing depth of amplified samples) (Fig. 2D–F). The median number of mosaic SNVs per patient identified by analysis of panel sequencing data was 223 from amplified samples versus 38 from unamplified samples, with variation among the amplified samples (SD 390.4 for amplified samples versus 3.3 for unamplified samples), suggesting that whole-genome amplification may randomly introduce artefacts that resemble mosaic variants. Thus, for panel analysis, we required candidate mosaic variants to be present in more than one electrode sample as DNA from more than one electrode sample for each patient was included on the panel (versus DNA from only one electrode sample per patient was included for ES and thus available for ES analysis). We also required orthogonal validation by amplicon sequencing. We detected and validated four deleterious mosaic variants in epilepsy-associated genes in three patients.

Identification of deleterious mosaic variants in epilepsy-associated genes from stereo-EEG electrode-derived DNA

Patient 5

Patient 5 is a 10-year-old boy with DRE who had onset of focal seizures with impaired awareness at 5 years of age.

Table 1 Patient cohort

Patient	Sex	Age (years)	Notable clinical findings	Surgical procedure/pathology	Number of electrodes	Brain tissue	Blood/ saliva
1	Female	12	Right parietal choroid plexus papilloma resected at 6 months with subsequent encephalomalacia and gliosis, seizure onset at 6 years	Resection/disconnection of right parieto-occipital seizure focus and right posterior corpus callosotomy; cerebral cortex and white matter with gliosis and reactive changes	16	Yes	Yes
2	Male	17	Seizure onset at 6 years, right frontal porencephalic cyst resected at 12 years with subsequent endoscopic third ventriculostomy	N/A	10	No	No
3	Female	18	DiGeorge syndrome, seizure onset at 11 years	Laser ablation of left posterior medial frontal seizure focus; N/A	15	No	Yes
4	Female	8	Left temporal cavernous malformation resected at ~3 years, seizure onset at 7 years	Left temporal lobectomy; cerebral cortex and white matter with gliosis, patchy neuronal dropout, occasional maloriented and ischaemic neurons and hippocampal sclerosis	12	Yes	Yes
5	Male	8	Seizure onset at 5 years, suspected left temporal/insular FCD	Laser ablation of left temporal operculo-insular seizure focus; N/A	16	No	Yes
6	Male	9	Seizure onset at 5 years, laser ablation of right subependymal heterotopia at 8 years, right hemiatrophy and suspected dysplasia, concern for atypical Rasmussen encephalitis	Laser ablation of right paracentral lobule and posterior insular seizure foci and needle biopsy of right superior parietal lobule; patchy neuronal loss and reactive astrogliosis	26	No	No
7	Male	10	Tuberous sclerosis complex, seizure onset at 2 months, large left frontal tuber conglomerate resected at 4 years	Resection of right temporal lobe and left frontal lobe tubers/seizure foci; cortical tubers	24	Yes	Yes
8	Male	11	Acute lymphocytic leukaemia diagnosed at 17 months s/p chemotherapy, seizure onset at 3 years, left mesial temporal sclerosis and calcifications	Laser ablation of left mesial temporal and parietal seizure focus; N/A	12	No	Yes
9	Female	10	Seizure onset at 2 years, left frontal resection at 5 years with FCD Ic on pathology	Laser ablation of left frontal seizure focus; N/A	15	No	Yes
10	Male	18	Transposition of the great arteries repaired as a neonate, seizure onset at 9 years, encephalomalacia	Laser ablation of left frontoparietal seizure focus; N/A	9	No	Yes

N/A, not applicable.

MRI demonstrated blurring of the grey and white matter interface in the left posterior insula and posterosuperior temporal gyrus, suggestive of an FCD (Fig. 3A and B). Clinical trio ES using buccal samples had revealed a maternally inherited variant of uncertain significance (VUS) in *HUWE1* (c.10667C>T, p.P3556L), which was determined not to be clinically relevant as the HUWE1-associated intellectual disability phenotype does not closely match his clinical features and does not include FCD. He underwent epilepsy surgery evaluation at 8 years of age, including sEEG with implantation of 16 left hemispheric electrodes (Fig. 3C). Multiple seizures were recorded, and the SOZ was localized to the left temporal-opercular-insular region, in/near the location of the suspected FCD (Fig. 3D). After multi-disciplinary discussion, the electrodes were removed, and he underwent imaging-guided LITT of the seizure focus (Fig. 3E). The ablated tissue included areas recorded by electrodes T1c Contacts 1–5, T1d Contacts 1–3, P1Ib Contacts 3–7 and P2d Contacts 1–5. He has remained seizure free in the 30 months since surgery.

For the 16 electrodes, electrode-derived amplified DNA concentrations ranged from 67.4 to 181 ng/µl, and unamplified DNA concentrations ranged from 2.57 to 12.7 ng/µl. We performed deep sequencing using amplified DNA from a subset of the electrodes, including the three electrodes corresponding to the SOZ, as well as unamplified DNA from a blood sample. A mosaic missense variant in *CNTNAP2* (NM_014141.6: c.3862C>T, p.R1288C) was detected in amplified DNA from 7/8 electrodes included on the panel with VAF ranging from 0.26 to 3.43%. This variant is rare (gnomAD[28] v4.1.0 allele frequency 4.4×10^{-5}) and predicted deleterious [Combined Annotation Dependent Depletion (CADD)[29] score 32]. Germline variants in *CNTNAP2* have been associated with an autosomal recessive neurodevelopmental disorder with epilepsy and cortical dysplasia (OMIM[30] 610042) and have been suggested to be

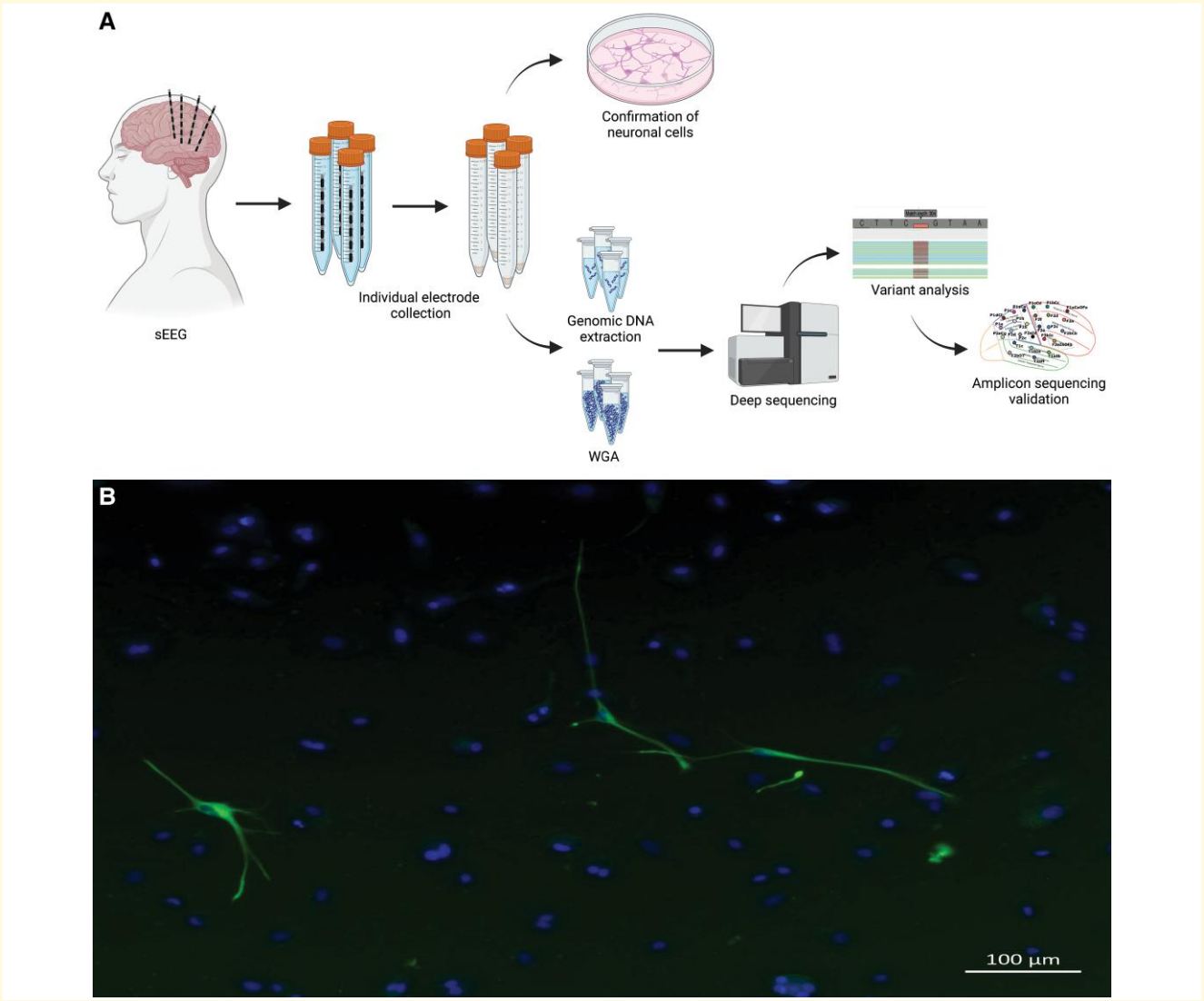

Figure 1 Study workflow and confirmation of neuronal cells adhered to sEEG electrodes. (**A**) Study workflow including sEEG procedure, individual electrode collection, confirmation of neuronal cells on electrodes, parallel extraction of genomic DNA and whole-genome amplification (WGA) from individual electrodes, deep sequencing, variant analysis, and amplicon sequencing validation of variants in DNA derived from individual electrodes. Created in BioRender (https://BioRender.com/s54s494). (**B**) Epifluorescence image of sEEG electrode-derived tissue cultured cells 2 days post-surgical removal with antibody labelling of microtubule-associated protein 2 (MAP2, green), a neuron-specific cytoskeletal protein isoform for identifying neuronal cells and visualization of dendritic processes. Nuclear staining was performed with Hoechst 33342 (blue).

associated with autosomal dominant epilepsy.[31] This variant has previously been reported in ClinVar[32] as a VUS (5 submissions) based on the American College of Medical Genetics and Genomics criteria[33] and in the literature as likely pathogenic in a patient with non-lesional focal epilepsy.[31] We performed subsequent amplicon sequencing using both amplified and unamplified DNA from multiple electrodes to validate and assess the distribution of the variant (Table 2). We validated the mosaic variant in amplified DNA from 9/16 electrodes and in unamplified DNA from 6/6 electrodes, including 5/6 electrodes corresponding to the SOZ and spread. The highest VAF was seen in samples from the T1c (2.01–3.43%) and P2aIc (3.25–3.43%) electrodes, corresponding to sites of the SOZ and ictal spread, respectively (Fig. 3F).

Patient 6

Patient 6 is an 11-year-old boy with a history of DRE who had seizure onset at 5 years of age. Multiple seizure types were described, including focal sensorimotor seizures and focal seizures with impaired awareness. He was initially diagnosed with a right temporal subependymal heterotopia, which was ablated at 8 years of age (Fig. 4A), resulting in several months of seizure freedom. Serial MRIs demonstrated progressive mild right cerebral hemispheric atrophy and dysplastic appearance of the right hemisphere, predominantly

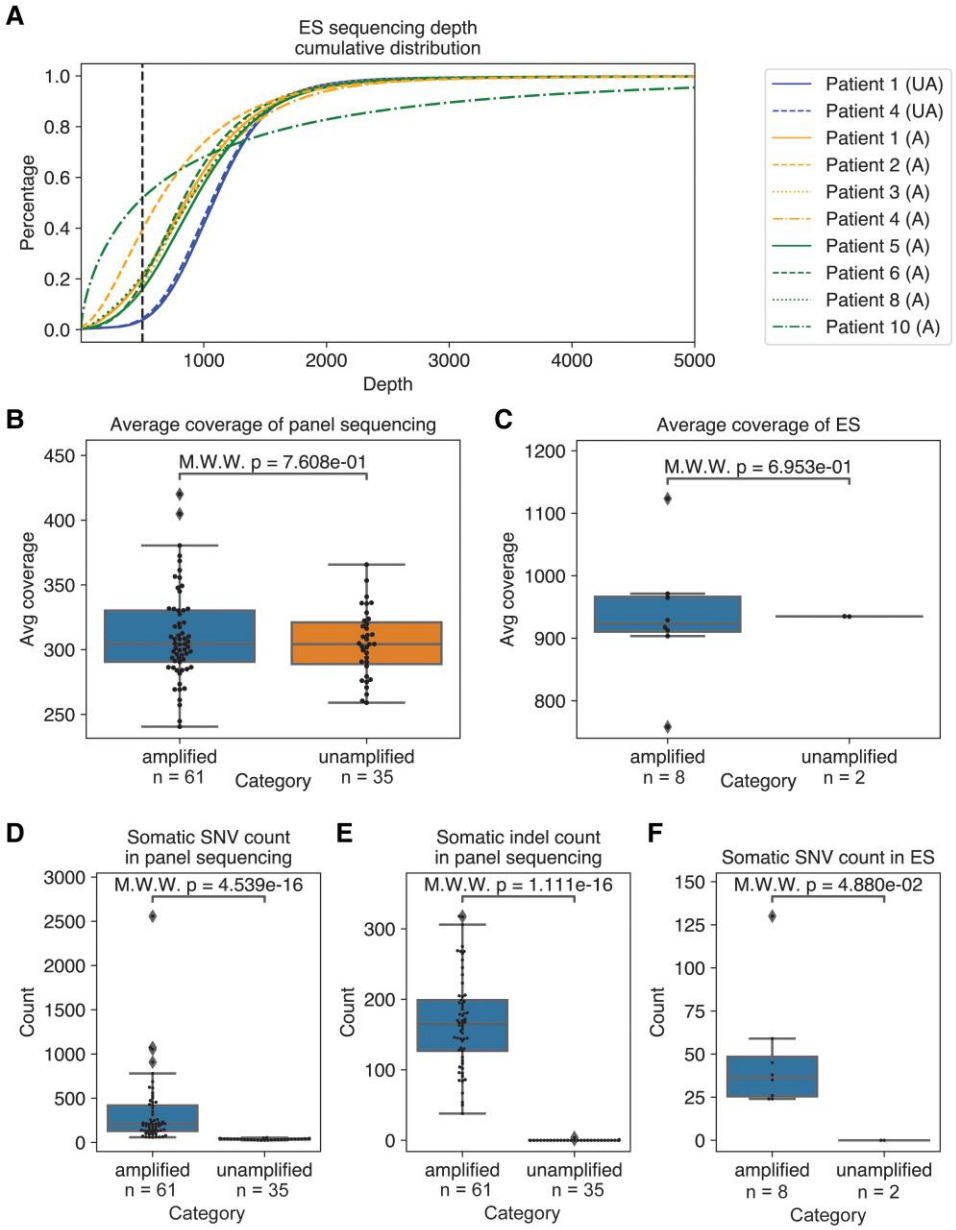

Figure 2 Deep sequencing coverage and variant calls. (**A**) The cumulative distribution of sequencing depth of all ES samples. The dashed line indicates the percentage of targeted regions that have been sequenced with 500× or less in each sample. The depth range is restricted to up to 5000× for visualization purposes. The average sequencing depth is not significantly different across amplified and unamplified samples in both panel sequencing ($P = 0.76$, **B**) and ES ($P = 0.70$, **C**). The number of mosaic variants is significantly higher in amplified samples than in unamplified samples for SNVs in panel sequencing ($P = 4.5 \times 10^{-16}$, **D**), indels in panel sequencing ($P = 1.1 \times 10^{-16}$, **E**) and SNVs in ES ($P = 0.049$, **F**). Avg, average; M.W.W., two-sided Mann–Whitney–Wilcoxon test with Bonferroni correction; A, whole-genome amplified; UA, unamplified.

involving the frontal, parietal, and to a lesser extent, temporal lobes without well-defined borders (Fig. 4B). Clinical ES using buccal samples was non-diagnostic.

In the setting of recurrent seizures, he underwent another epilepsy surgery evaluation at 9 years of age, including sEEG with implantation of 26 right hemispheric electrodes (Fig. 4C). Four seizure types were recorded: (I) epilepsia partialis continua (EPC) of the left foot, (II) focal motor seizures involving his left hemibody, (III) focal seizures with impaired awareness, and (IV) choking/gagging episodes. Seizure Types I and II had presumed seizure onset focus in the right mesial paracentral lobule, while seizure Type III involved the right anterior frontal/orbito-frontal lobe, and seizure Type IV involved the right posterior insula. After multi-disciplinary discussion, the electrodes were removed, and he underwent LITT of the seizure foci, including regions recorded by electrodes F1bCc Contacts 5–11, F1cCd Contacts 1–5, P1aCe Contacts 2–8, P1c Contacts 1–8, P2aId Contacts 1–4 and F3bIc Contact 1. Pathology

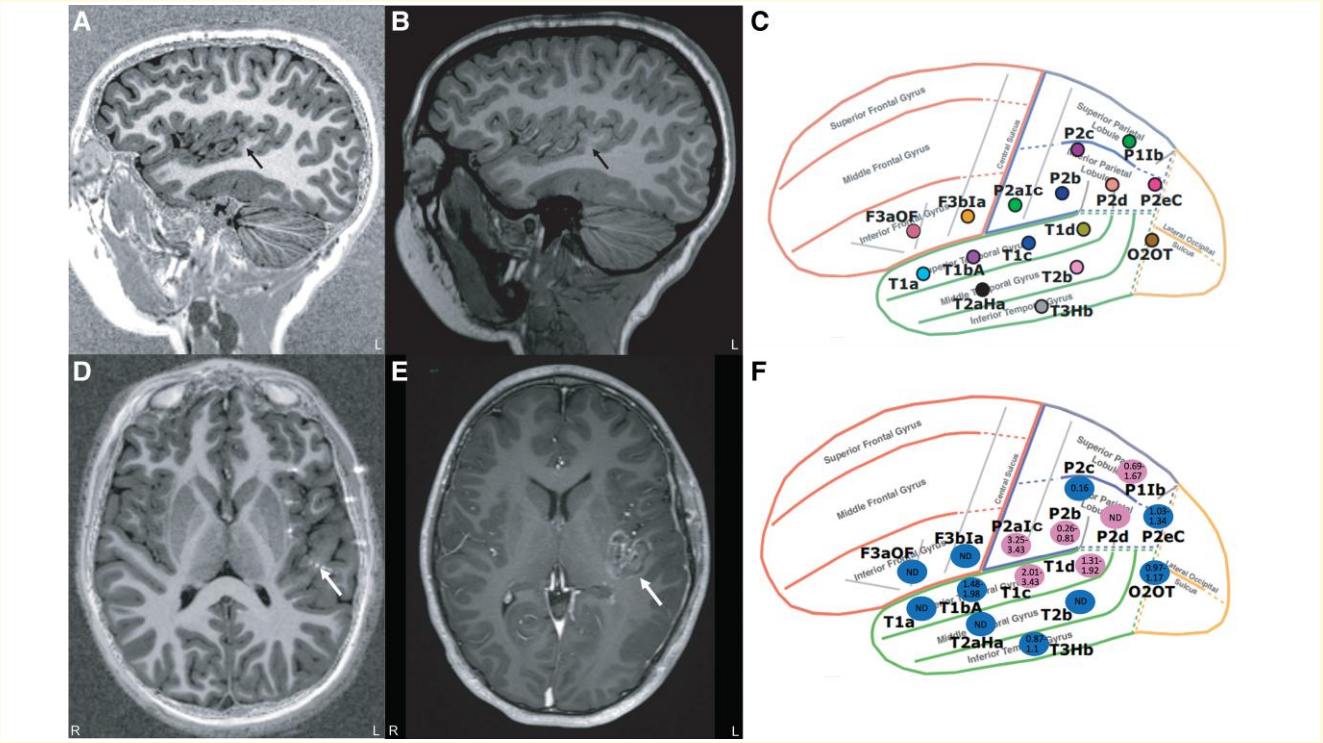

Figure 3 MRI, sEEG electrode placement, and *CNTNAP2* variant mosaic gradient for Patient 5. Blurring of the grey and white matter interface in the left posterior insula and posterior superior temporal gyrus (arrows) on (**A**) sagittal magnetization prepared rapid acquisition gradient echo with two inversion times (MP2RAGE) and (**B**) conventional sagittal magnetization prepared rapid acquisition gradient echo (MPRAGE) images. (**C**) Lateral view of the sEEG electrode implantation plan for Patient 5 using the standardized electrode nomenclature for stereo-EEG applications (SENSA) naming system. (**D**) Axial fused MP2RAGE and CT image with one of the active sEEG electrodes in the suspected areas overlaid on the MP2RAGE image. (**E**) Axial post-LITT ablation post-contrast MPRAGE shows the treated area, which matches the abnormality seen on prior MRIs. (**F**) sEEG plan overlaid with the mosaic gradient of the detected *CNTNAP2* variant. Pink ovals represent electrodes corresponding to seizure onset or spread, and blue ovals represent non-involved electrodes. The number in each oval is the VAF detected in DNA extracted from that electrode. L, left; ND, not detected; R, right.

demonstrated patchy neuronal loss and displaced neurons with reactive astrogliosis. There was transient improvement in seizures following LITT, especially of EPC, but on the most recent follow-up 6 months post-surgery, he has had recurrence of EPC and persistence of the other baseline seizure types.

For the 26 electrodes, amplified DNA concentrations ranged from 135 to 193 ng/μl and unamplified DNA concentrations ranged from 1.49 to 7.51 ng/μl. Deep sequencing using amplified DNA from a subset of the electrodes detected two deleterious mosaic variants (Table 3). First, we detected a mosaic missense variant in *CIC* (NM_001386298.1: c.4723C>T, p.R1575C) in amplified DNA from 3/4 electrodes included on the panel with VAF ranging from 1.6 to 5.13%. This variant is rare (gnomAD allele frequency 1.6×10^{-5}), predicted deleterious (CADD score 25.1), and has previously been reported in COSMIC[34] (melanoma). Variants in *CIC* have been associated with an autosomal dominant intellectual disability disorder with seizures in some patients (OMIM 617600). We validated the mosaic variant in amplified DNA from 25/26 electrodes and in unamplified DNA from 10/11 electrodes, including 14/14 electrodes corresponding to sites with active ictal activity and ictal spread for the four seizure types.

Second, we detected a mosaic missense variant in *PTEN* (NM_000314.8: c.333G>T, p.W111C) in amplified DNA from 4/4 electrodes included on the panel with VAF ranging from 0.88 to 2.6%. This variant is rare (gnomAD allele frequency 6.2×10^{-7}), predicted deleterious (CADD score 32) and a different variant at the same amino acid position (c.331T>C, p.W111R) is reported as pathogenic/likely pathogenic in ClinVar. PTEN is a negative regulator of the mTOR pathway, and variants in *PTEN* have been associated with a range of overgrowth disorders including some patients with seizures and MCDs.[1] We validated the mosaic *PTEN* variant in amplified DNA from 3/3 electrodes and in unamplified DNA from 1/1 electrode, including 3/3 electrodes corresponding to sites with active ictal activity for the four seizure types.

Patient 10

Patient 10 is a 19-year-old man with DRE who had seizure onset at 9 years of age. His seizures begin with a non-specific sensory aura followed by impaired awareness and motor involvement of his right arm, at times with evolution to bilateral tonic-clonic seizures. His medical history is notable for

Table 2 VAF for CNTNAP2 variant detected in Patient 5

Electrode	Source	Panel VAF (%)	Amplicon VAF (%)	Source	Amplicon VAF (%)
Electrodes corresponding to presumed seizure onset focus					
T1c	Amplified DNA	3.43	2.01	Unamplified DNA	
T1d	Amplified DNA	1.36	1.92	Unamplified DNA	1.31
P2d	Amplified DNA	Not detected	Not detected	Unamplified DNA	
Electrodes corresponding to seizure spread					
P2alc	Amplified DNA	3.25	3.43	Unamplified DNA	
P2b	Amplified DNA	0.26	0.81	Unamplified DNA	
P1lb	Amplified DNA	0.69	1.18	Unamplified DNA	1.67
Other electrodes					
T1a	Amplified DNA		Not detected	Unamplified DNA	
T1bA	Amplified DNA	1.98	Not detected	Unamplified DNA	1.48
T2aHa	Amplified DNA		Not detected	Unamplified DNA	
T2b	Amplified DNA		Not detected	Unamplified DNA	
T3Hb	Amplified DNA		0.87	Unamplified DNA	1.1
P2c	Amplified DNA		0.16	Unamplified DNA	
P2eC	Amplified DNA	1.34	1.03	Unamplified DNA	1.03
O2OT	Amplified DNA		1.17	Unamplified DNA	0.97
F3aOF	Amplified DNA		Not detected	Unamplified DNA	
F3bla	Amplified DNA		Not detected	Unamplified DNA	
Blood	Unamplified DNA	Not detected			

transposition of the great arteries, repaired in the neonatal period. MRI showed left posterior frontal and right parietal encephalomalacia, though likely to represent remote embolic infarctions (Fig. 4D and E). Given this presentation, he received a diagnosis of acquired focal epilepsy and did not undergo clinical genetic testing. He underwent pre-surgical evaluation at 18 years of age, and his non-invasive data were concordant with the left-sided lesion, leading to sEEG with implantation of 9 left hemispheric electrodes (Fig. 4F). Multiple habitual seizures were recorded with onset in the left opercular insular region immediately deep and lateral to one of the encephalomalacia foci. After multidisciplinary discussion, the electrodes were removed and he underwent LITT of the seizure focus. The ablated tissue included areas recorded by electrodes F2a Contact 1, F2b Contacts 1–2, F3a Contact 8, F3bI Contacts 1–8, and P2a Contacts 2–5. He was seizure free for 6 months post-surgery and then had recurrence of seizures that continued to be refractory to ASM treatment. He underwent an additional laser ablation at 19 years of age to slightly expand the ablation volume, which included areas recorded by electrodes F2a, F2b, F3a, and F3bI. He had improvement in seizure frequency for 6 months and then again had recurrence of seizures, with plans for an additional sEEG implantation.

For the 9 electrodes from his initial sEEG implantation, amplified DNA concentration ranged from 17.1 to 95.1 ng/μl and unamplified DNA concentration ranged from 2.94 to 7.2 ng/μl. Deep ES using amplified DNA from one of the electrodes detected a predicted deleterious mosaic variant in *KDM6A* (NM_001291415.2: c.3203G>A, p.G1068E) in the electrode F3bI, an initial site of ictal activity during the Phase II recordings, at a VAF of 1.63% (Table 4). This variant is rare (not present in gnomAD) and predicted deleterious (CADD score 26.5). Variants in *KDM6A* have been associated with Kabuki syndrome 2 (OMIM 300867), which is characterized by intellectual disability, seizures, congenital heart disease (cardiac tissue was not available) and dysmorphic features. The variant validated in amplified DNA from 1/5 electrodes (F3bI) at a VAF of 1.13% and did not validate in unamplified DNA from 2/2 assessed electrodes or from blood.

Detection of pathogenic germline variants

We detected previously identified germline variants in two patients. Patient 7 has DRE in the setting of TSC. We detected a clinically known germline *TSC2* frameshift variant in all sequenced samples. Though TSC lesions are thought to occur due to the presence of local, tissue-specific mosaic second variants (so-called 'second hits'), we did not identify a mosaic variant in the amplified DNA from electrodes, unamplified DNA from electrodes, or unamplified DNA from resected brain tissue (tuber) samples. Patient 9 has DRE in the setting of FCD Ic demonstrated on pathology from a previous resection. We detected a clinically known germline *DEPDC5* missense variant in all sequenced samples, but despite reports of a similar second hit phenomenon for focal lesions in patients with germline *DEPDC5* variants,[35] we did not identify a second mosaic variant in amplified DNA from electrodes. No resected brain tissue was available as the patient underwent ablation with LITT.

Discussion

The past decade has seen increasing recognition of the important role of brain somatic mosaicism in focal DRE, initially in lesional and more recently in non-lesional cases, involving genes in the mTOR pathway and more recently recognized contributors, including *SLC35A2*.[36-38]

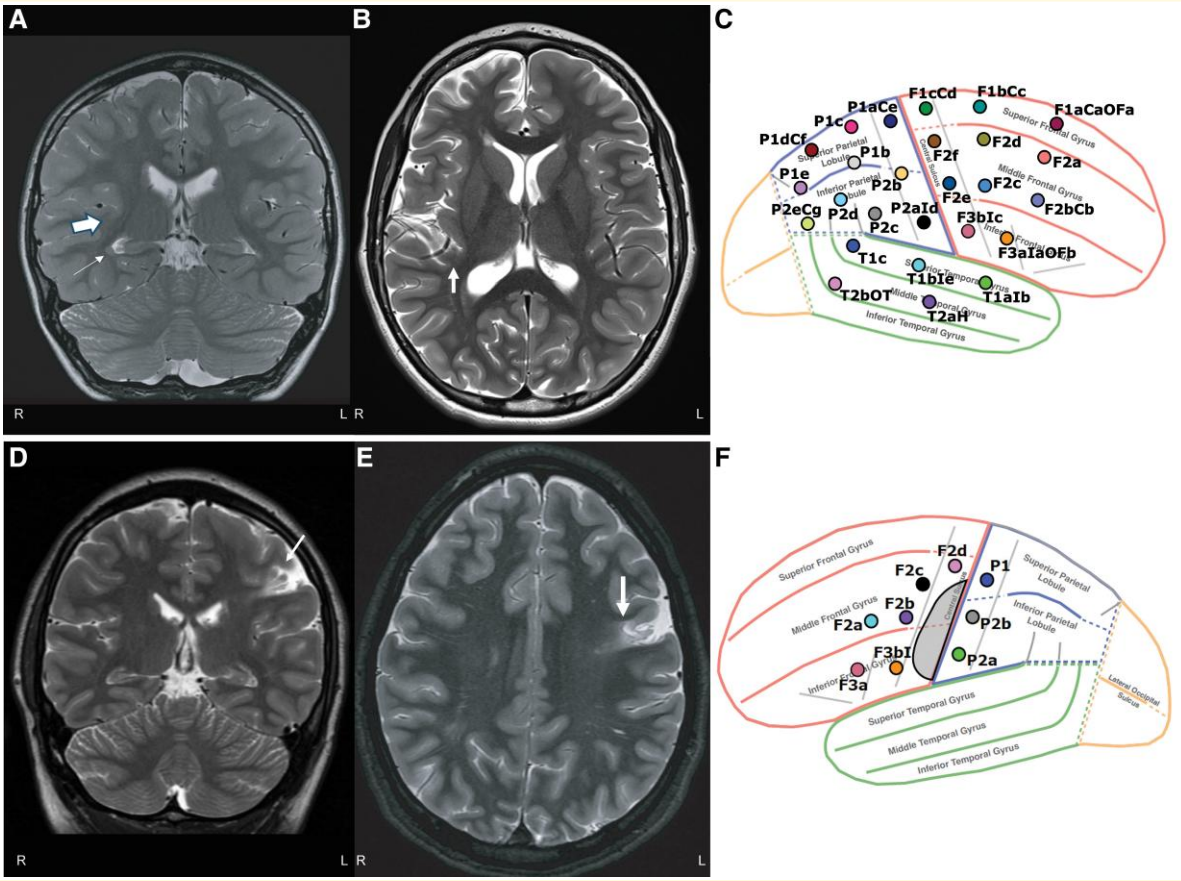

Figure 4 MRI and sEEG electrode placement for Patients 6 and 10. (**A**) Coronal T2-weighted MRI from an outside hospital for Patient 6 shows subependymal grey matter heterotopia adjacent to the right temporal horn (thin arrow) and subtle blurring of the grey and white matter interface in the right posterior insula and posterosuperior temporal gyrus (thick arrow). (**B**) Subsequent axial T2-weighted MRI obtained at our institution after the heterotopia had been ablated at the referring institution and before sEEG placement, again showing the subtle blurring at the grey and white matter interface in the right posterior insula (thick arrow) and right frontoparietal-predominant cerebral atrophy. (**C**) Lateral view of the sEEG electrode implantation plan for Patient 6 using the SENSA naming system. Coronal (**D**) and axial (**E**) T2-weighted MRI for Patient 10 show encephalomalacia in the left frontal lobe. (**F**) Lateral view of the sEEG electrode implantation plan for Patient 10 using the SENSA naming system. The shaded grey area represents the area of encephalomalacia. L, left; R, right.

These discoveries have relied on access to surgically resected brain tissue samples. We do not know the contribution of somatic mosaic variants in patients with DRE who are ineligible for surgery or have less invasive surgical interventions that do not involve an open craniotomy. The evolving practice of seizure localization using sEEG electrodes provides unique access to small amounts of adherent DNA from these electrodes and the ability to correlate the presence and VAF of genetic variants from specific brain loci with the ictal and inter-ictal findings in a given patient. In this study, we enrolled 10 paediatric patients with DRE undergoing sEEG implantation at our institution and aimed to detect mosaic variants in DNA extracted from the trace brain tissue recovered from the explanted sEEG electrodes, to assess the VAFs across electrodes placed in several brain regions, and to compare the feasibility of detection and validation of mosaic variants between amplified and unamplified electrode–derived DNA. In total, from these 10 individuals, we extracted amplified and unamplified DNA in parallel from over 150 individual electrodes and used deep sequencing approaches to discover and validate 4 mosaic variants in electrode-derived DNA from 3 patients who underwent laser ablation and did not have resected brain tissue samples available, in addition to the previously reported mosaic *PIK3CA* variant in an eleventh patient who did have resected brain tissue available.[16]

The use of explanted sEEG electrodes as a source of brain-derived DNA was first reported by Montier *et al.*[10] in 2019, who identified a mosaic frameshift variant in *MEN1* in a patient with DRE and periventricular nodular heterotopia using whole-genome amplified DNA from pooled sEEG electrodes. The variant was detected at a relatively high VAF (16.7%) in the electrode-derived DNA, which allowed validation by Sanger sequencing. The authors note that the variant was not reported in previous ES (read depth not reported) using blood-derived DNA or detected in Sanger sequencing using blood-derived DNA. Subsequently, Ye *et al.*[9] identified a mosaic nonsense variant in *KCNT1* in a patient

Table 3 VAF for CIC and PTEN variants detected in Patient 6

Electrode	Source	Panel VAF (%)	Amplicon VAF (%)	Source	Amplicon VAF (%)
CIC variant					
Electrodes corresponding to presumed seizure onset focus					
F1bCc[a]	Amplified DNA		1.55	Unamplified DNA	
F1cCd[a]	Amplified DNA	5.13	4.68	Unamplified DNA	Not detected
F3blc [a,b]	Amplified DNA		0.83	Unamplified DNA	
P1aCe[a]	Amplified DNA		2.3	Unamplified DNA	
P1c[a]	Amplified DNA		1.52	Unamplified DNA	
F1aCaOFa[c]	Amplified DNA		5.65	Unamplified DNA	
F3alaOFb[c]	Amplified DNA	3.02	2.51	Unamplified DNA	2.69, 2.62
P2ald[d]	Amplified DNA	1.6	0.78	Unamplified DNA	4.53
Electrodes corresponding to seizure spread					
F2a[e]	Amplified DNA	Not detected	Not detected	Unamplified DNA	3.24
F2bCb[e]	Amplified DNA		3.49	Unamplified DNA	
F2c[e]	Amplified DNA		2.05	Unamplified DNA	
P1dCf[e]	Amplified DNA		2.45	Unamplified DNA	3.12
T1alb[e]	Amplified DNA		1.54	Unamplified DNA	
T2aH[e]	Amplified DNA		5.61	Unamplified DNA	
Other Electrodes					
F2d	Amplified DNA		9.64	Unamplified DNA	
F2e	Amplified DNA		2.96	Unamplified DNA	2.4
F2f	Amplified DNA		2.27	Unamplified DNA	
P1b	Amplified DNA		3.1	Unamplified DNA	3.33
P1e	Amplified DNA		2.07	Unamplified DNA	
P2b	Amplified DNA		3.21	Unamplified DNA	
P2c	Amplified DNA		3.5	Unamplified DNA	2.71
P2d	Amplified DNA		3.71	Unamplified DNA	
P2eCg	Amplified DNA		3.95	Unamplified DNA	3.98
T1ble	Amplified DNA		2.78	Unamplified DNA	2.97
T1c	Amplified DNA		3.87	Unamplified DNA	
T2bOT	Amplified DNA		1.24	Unamplified DNA	2.49
PTEN variant					
Electrodes corresponding to presumed seizure onset focus					
F1cCd[a]	Amplified DNA	1.26	0.42	Unamplified DNA	
F3alaOFb[c]	Amplified DNA	1.45	0.44	Unamplified DNA	0.38
P2ald[d]	Amplified DNA	2.6	0.44	Unamplified DNA	
Electrodes corresponding to seizure spread					
F2a[e]	Amplified DNA	0.88		Unamplified DNA	

[a]Corresponding to presumed seizure onset focus and spread for seizure Types I (left foot EPC) and II (focal motor seizures involving left hemibody). [b]Corresponding to seizure spread for seizure Type IV (choking/gagging). [c]Corresponding to presumed seizure onset focus for seizure Type III (focal seizure with impaired awareness). [d]Corresponding to presumed seizure onset focus for seizure Type IV (choking/gagging). [e]Corresponding to seizure spread for seizure Type III (focal seizure with impaired awareness).

Table 4 VAF for KDM6A variant detected in Patient 10

Electrode	Source	Exome VAF (%)	Amplicon VAF (%)	Source	Amplicon VAF (%)
Electrodes corresponding to presumed seizure onset focus					
F3a	Amplified DNA		Not detected	Unamplified DNA	Not detected
F3bl	Amplified DNA	1.63	1.13	Unamplified DNA	
Other electrodes					
F2a	Amplified DNA		Not detected	Unamplified DNA	
P1	Amplified DNA		Not detected	Unamplified DNA	
F2c	Amplified DNA		Not detected	Unamplified DNA	Not detected
Blood	Unamplified DNA		Not detected		

with multi-focal DRE, also using whole-genome amplified DNA from pooled sEEG electrodes. However, by collecting the electrodes into three regional pools, they were able to demonstrate a VAF gradient, with the highest VAF in the most epileptogenic region. Klein *et al.*[14,39] recently reported identification and validation of a mosaic *MTOR* variant in a patient with DRE and FCD using whole-genome amplified DNA from neuronal nuclei isolated from pooled electrodes in the lesion/SOZ. The variant was not detected in neuronal nuclei from pooled electrodes outside the lesion, in astrocyte nuclei, or in saliva. In these case reports, the mosaic variants were detected and validated using only amplified DNA, as unamplified DNA was not extracted from the electrodes and resected brain tissue was not available. In addition, these

groups used DNA extracted from pooled sEEG electrodes, limiting the resolution of the genetic findings. The presence of the *MEN1* mosaic variant in the first report was not thought to necessarily have a causal role for the individual's epilepsy, whereas the presence of the *KCNT1* and *MTOR* mosaic variants in the latter reports were thought to have been contributing to the individuals' epilepsy given the established roles of these genes in epilepsy.

Checri *et al.*[12] reported detection of somatic mosaic variants, which were previously identified in resected brain tissue samples, in unamplified DNA from individual sEEG electrodes in patients with DRE and FCDIIa who underwent additional pre-surgical evaluations. In their first patient, the previously identified variant was detected in 3/9 assessed electrodes, all in the epileptogenic zone; in their second patient, the variant was not detected in any of the 12 assessed electrodes, and in their third patient, the variant was detected in 1/11 assessed electrodes, which was in the seizure propagation zone. The authors reported similarly low concentrations of unamplified DNA (0.2–3.9 ng/μl) from the 38 electrodes they extracted as we report here from the >150 electrodes for which we performed DNA extraction. As in our prior report of a mosaic *PIK3CA* variant, the study by Checri *et al.*[12] reported detection of variants in electrode-derived DNA that had already been identified in resected brain tissue. Similarly, Gatesman *et al.*[15] recently reported identification of a mosaic *FGFR1* variant from one sEEG electrode and a resected brain tissue sample in a patient with a low-grade epilepsy-associated tumour (validation was not reported). In contrast, we now report identification and validation of new variants in electrode-derived DNA in patients who did not have resected brain tissue available.

We demonstrate the ability to consistently recover trace brain tissue and extract DNA from individual sEEG electrodes and to identify and validate deleterious mosaic variants in amplified and unamplified electrode–derived DNA. When analysing deep sequencing data for mosaic variants, we observed that sequencing data from amplified DNA samples resulted in a significantly higher number of called mosaic variants compared with unamplified DNA samples, in the setting of similar depth of coverage, suggesting that whole-genome amplification may introduce artefacts and that sequencing of multiple independent samples from the same individual may help distinguish true somatic mutation from random artefact. When validating candidate mosaic variants, we observed that validation in amplified versus unamplified DNA from the same electrode is not always consistent—we show examples of detection in amplified but not unamplified DNA from the same electrode and vice versa. When we were able to detect the variant in both sources, the VAF was relatively similar. In our recent case report, we were unable to detect a disease-causing *PIK3CA* mosaic variant, which was identified in resected brain tissue–derived DNA, in unamplified electrode–derived DNA, although we were able to detect the variant in amplified electrode–derived DNA in 4/17 electrodes.[16] Moreover, although in this study we were able to detect previously known pathogenic germline SNVs in amplified electrode–derived DNA, we anecdotally observed that the VAF varied across samples (e.g. for the germline *DEPDC5* variant, the VAF ranged from 28.6 to 85.6% in the amplified electrode–derived DNA samples and was called as mosaic, germline heterozygous, and germline homozygous depending on the sample; the VAF was 44.6% and called as germline heterozygous in unamplified blood-derived DNA). We were unable to detect a previously known pathogenic germline copy number variant (CNV) in amplified electrode–derived DNA (Patient 3). Thus, although whole-genome amplification of electrode–derived DNA provides more DNA for downstream experiments, future optimization of techniques is needed. We believe extraction of unamplified DNA is important, particularly for patients where another source of unamplified brain-derived DNA (e.g. resected brain tissue) is not available, if electrode-derived DNA is to be used for clinical molecular genetic diagnosis and decision-making.

In addition to our previously reported mosaic *PIK3CA* variant in a patient who underwent sEEG and resection, we discovered and validated a total of four deleterious mosaic variants in epilepsy-associated genes using electrode-derived DNA in three patients who underwent sEEG and LITT. In Patient 5 with DRE in the setting of an FCD, we were able to assess the *CNTNAP2* VAF distribution across amplified DNA from 16/16 electrodes and unamplified DNA from 6/16 electrodes. The *CNTNAP2* variant was detected in 2/3 electrodes corresponding to region of ictal onset and in 3/3 electrodes corresponding to seizure spread, with a relationship between the level of mosaicism and epileptogenic network suggested at single electrode resolution. Germline variants in *CNTNAP2* have been associated with an autosomal recessive neurodevelopmental disorder with epilepsy and cortical dysplasia as well as reported in autosomal dominant epilepsy; the same variant in a germline state has been reported as likely pathogenic in a patient with non-lesional focal epilepsy.[31] Although additional evidence is needed for autosomal dominant *CNTNAP2*-related disease to conclude that this mosaic variant is disease-contributory or causative, we demonstrate the ability to discover deleterious mosaic variants in epilepsy-associated genes from individual sEEG electrodes as well as validate in amplified and unamplified DNA from single electrodes. In Patient 6, who had multiple seizure types and foci in the setting of a MCD, we validated two deleterious mosaic variants in *CIC* and *PTEN*. Germline variants in *CIC* have been associated with an autosomal dominant intellectual disability disorder with seizures in some patients,[40] and germline variants in *PTEN* have been associated with a range of overgrowth phenotypes including MCDs and epilepsy.[41,42] Given the relatively low VAF for the *PTEN* mosaic variant, we believe it is possible that it could be contributing to the dysplastic nature of the right hemisphere without frank macrocephaly. It is interesting to speculate if multiple mosaic variants with different distributions may contribute to epilepsy pathogenesis in patients with multi-focal epilepsy, and future work is needed to investigate this hypothesis. In Patient 10, who had

DRE in the setting of encephalomalacia and a history of repaired congenital heart disease, a fourth mosaic variant was detected in *KDM6A*. Germline variants in *KDM6A* have been associated with Kabuki syndrome 2, which is characterized by intellectual disability, seizures, congenital heart disease, and dysmorphic features. We did not have cardiac tissue available (although the variant was not detected in blood-derived DNA), and we were able to validate the variant in the same amplified DNA sample but not the few available unamplified DNA samples from single electrodes and thus are cautious about the accuracy and clinical relevance of this finding.

Overall, our study demonstrates the potential utility of sequencing sEEG electrode-derived DNA as a minimally invasive genetic diagnostic approach for patients with unexplained epilepsy. This increasingly available albeit small-quantity source of DNA may be especially relevant for those individuals with DRE who are not eligible for or choose not to undergo surgical resection and thus do not have resected brain tissue available for mosaic variant assessment. We provide the first report of mosaic variant discovery using DNA derived from individual sEEG electrodes, compare amplified and unamplified electrode-derived DNA, and provide further evidence for a relationship between the degree of mosaicism, reflected in the VAF, and the degree of abnormal electrical network activity, specifically proximity to the SOZ and seizure propagation zone.

Our study has limitations, notably the relatively small number of patients and the heterogeneity of patient phenotypes, and requires validation in larger cohorts. Further, as previously noted,[12] each sEEG electrode has multiple contacts and passes through multiple brain regions when being implanted and explanted; thus, the cells that are attached to even a single electrode may come from distinct brain regions with different electrophysiological activity. Further optimization of electrode design and DNA extraction, deep sequencing, and mosaic variant analysis techniques should continue to improve the sensitivity and specificity of this approach. Finally, given the relatively recent discovery of the role of mosaic variants in epilepsy-related brain lesions, our ability to ascribe causality to the mosaic variants we report in this study is limited and will require additional efforts in somatic variant curation.[43] Human and animal model studies have demonstrated that VAFs of 1% and even lower (e.g. as low as 0.04%) are sufficient to cause seizures in certain contexts, and further studies on the VAF threshold leading to pathogenicity are also needed.[7,37,44]

In the future, the minimally invasive approach we describe here holds promise for advancing precision diagnosis, which may one day become sensitive and reliable enough to implement rapidly such that the resulting data could be incorporated into the surgical decision-making process for patients with DRE. Additionally, by providing precision diagnoses, sEEG electrode-derived DNA and analysis for mosaic variants may guide surgical planning ('genetic margins') and post-surgical prognosis using genetic data at single electrode resolution and may guide precision therapies for patients who do not undergo resection. Precision therapies are already emerging for patients with DRE and mosaic variants in mTOR pathways genes, and establishing precision diagnoses will be critical for eligibility for future clinical trials of precision therapies.[1,45]

Supplementary material

Supplementary material is available at *Brain Communications* online.

Acknowledgements

We thank the patients and their families who enrolled in this study. The graphical abstract was created in BioRender (https://BioRender.com/t58c673).

Funding

A.M.D. was supported by the National Institute of Child Health and Human Development (T32 HD098061). H.W.P. was supported by the National Institute of Neurological Disorders and Stroke (R25 NS079198) and by Credit Unions Kids at Heart. E.A.L. and Y.W. were supported by Allen Discovery Center programme, a Paul G. Allen Frontiers Group advised programme of the Paul G. Allen Family Foundation. R.S.S. was supported by the National Institute of Neurological Disorders and Stroke (R00 NS112604). A.Y.H. was supported by the National Institute on Aging (R56 AG079857 and R01 AG088082) and Alzheimer's Association Research Fellowship (AARF-22-972287). C.A.W. was supported by the National Institute of Neurological Disorders and Stroke (R01NS035129 and R01NS032457), the Simons Foundation and Autism BrainNet (953759), the Allen Discovery Center and grant 62587 from the John Templeton Foundation. (The opinions expressed in this publication are those of the author(s) and do not necessarily reflect the views of the John Templeton Foundation.) C.A.W. is an investigator of the Howard Hughes Medical Institute. This research was supported in part by the Boston Children's Hospital Rosamund Stone Zander Translational Neuroscience Center Human Neuron Core Repository for Neurological Disorders, Credit Unions Kids at Heart and the Intellectual and Developmental Disabilities Research Center [National Institute of Child Health and Human Development (P30 HD018655)].

Competing interests

The authors report no competing interests.

Data availability

The code used for this study is publicly available at https://github.com/ElainW/SEEG. The sequencing data that support the findings of this study are available from the corresponding author, upon reasonable request.

References

1. D'Gama AM, Poduri A. Precision therapy for epilepsy related to brain malformations. *Neurotherapeutics*. 2021;18(3):1548-1563.
2. Blumcke I, Spreafico R, Haaker G, *et al.* Histopathological findings in brain tissue obtained during epilepsy surgery. *N Engl J Med*. 2017;377(17):1648-1656.
3. Lopez-Rivera JA, Leu C, Macnee M, *et al.* The genomic landscape across 474 surgically accessible epileptogenic human brain lesions. *Brain*. 2023;146(4):1342-1356.
4. Winawer MR, Griffin NG, Samanamud J, *et al.* Somatic SLC35A2 variants in the brain are associated with intractable neocortical epilepsy. *Ann Neurol*. 2018;83(6):1133-1146.
5. D'Gama AM, Walsh CA. Somatic mosaicism and neurodevelopmental disease. *Nat Neurosci*. 2018;21(11):1504-1514.
6. Poduri A, Evrony GD, Cai X, Walsh CA. Somatic mutation, genomic variation, and neurological disease. *Science*. 2013;341(6141):1237758.
7. D'Gama AM, Poduri A. Brain somatic mosaicism in epilepsy: Bringing results back to the clinic. *Neurobiol Dis*. 2023;181:106104.
8. Ye Z, Chatterton Z, Pflueger J, *et al.* Cerebrospinal fluid liquid biopsy for detecting somatic mosaicism in brain. *Brain Commun*. 2021;3(1):fcaa235.
9. Ye Z, Bennett MF, Neal A, *et al.* Somatic mosaic mutation gradient detected in trace brain tissue from stereo-EEG depth electrodes. *Neurology*. 2022;99(23):1036-1041.
10. Montier L, Haneef Z, Gavvala J, *et al.* A somatic mutation in MEN1 gene detected in periventricular nodular heterotopia tissue obtained from depth electrodes. *Epilepsia*. 2019;60(10):e104-e109.
11. Kim S, Baldassari S, Sim NS, *et al.* Detection of brain somatic mutations in cerebrospinal fluid from refractory epilepsy patients. *Ann Neurol*. 2021;89(6):1248-1252.
12. Checri R, Chipaux M, Ferrand-Sorbets S, *et al.* Detection of brain somatic mutations in focal cortical dysplasia during epilepsy presurgical workup. *Brain Commun*. 2023;5(3):fcad174.
13. Ye Z, Bennett MF, Bahlo M, *et al.* Cutting edge approaches to detecting brain mosaicism associated with common focal epilepsies: Implications for diagnosis and potential therapies. *Expert Rev Neurother*. 2021;21(11):1309-1316.
14. Klein KM, Mascarenhas R, Merrikh D, *et al.* Identification of a mosaic MTOR variant in purified neuronal DNA in a patient with focal cortical dysplasia using a novel depth electrode harvesting technique. *Epilepsia*. 2024;65(6):1768-1776.
15. Gatesman TA, Hect JL, Phillips HW, *et al.* Characterization of low-grade epilepsy-associated tumor from implanted stereoelectroencephalography electrodes. *Epilepsia Open*. 2024;9(1):409-416.
16. Phillips HW, D'Gama AM, Wang Y, *et al.* Somatic mosaicism in PIK3CA variant correlates with stereoelectroencephalography-derived electrophysiology. *Neurol Genet*. 2024;10(1):e200117.
17. Stone S, Madsen JR, Bolton J, Pearl PL, Chavakula V, Day E. A standardized electrode nomenclature for stereoelectroencephalography applications. *J Clin Neurophysiol*. 2021;38(6):509-515.
18. Smith RS, Kenny CJ, Ganesh V, *et al.* Sodium channel SCN3A (Na(V)1.3) regulation of human cerebral cortical folding and oral motor development. *Neuron*. 2018;99(5):905-913 e7.
19. D'Gama AM, Woodworth MB, Hossain AA, *et al.* Somatic mutations activating the mTOR pathway in dorsal telencephalic progenitors cause a continuum of cortical dysplasias. *Cell Rep*. 2017;21(13):3754-3766.
20. Huang AY, Zhang Z, Ye AY, *et al.* MosaicHunter: Accurate detection of postzygotic single-nucleotide mosaicism through next-generation sequencing of unpaired, trio, and paired samples. *Nucleic Acids Res*. 2017;45(10):e76.
21. Dunn T, Berry G, Emig-Agius D, *et al.* Pisces: An accurate and versatile variant caller for somatic and germline next-generation sequencing data. *Bioinformatics*. 2019;35(9):1579-1581.
22. Li H, Durbin R. Fast and accurate short read alignment with Burrows-Wheeler transform. *Bioinformatics*. 2009;25(14):1754-1760.
23. Van der Auwera GA, O'Connor BD, eds. *Genomics in the cloud: Using Docker, GATK, and WDL in Terra*. 1st ed. O'Reilly Media; 2020.
24. Broad Institute, Picard Toolkit. Accessed 4 August 2023, https://broadinstitute.github.io/picard/
25. Quinlan AR, Hall IM. BEDTools: A flexible suite of utilities for comparing genomic features. *Bioinformatics*. 2010;26(6):841-842.
26. Robinson JT, Thorvaldsdottir H, Winckler W, *et al.* Integrative genomics viewer. *Nat Biotechnol*. 2011;29(1):24-26.
27. Virtanen P, Gommers R, Oliphant TE, *et al.* SciPy: open source scientific tools for Python. *Nat Methods*. 2020;17(3):261-272.
28. Karczewski KJ, Francioli LC, Tiao G, *et al.* The mutational constraint spectrum quantified from variation in 141,456 humans. *Nature*. 2020;581(7809):434-443.
29. Kircher M, Witten DM, Jain P, O'Roak BJ, Cooper GM, Shendure J. A general framework for estimating the relative pathogenicity of human genetic variants. *Nat Genet*. 2014;46(3):310-315.
30. Online Mendelian Inheritance in Man, OMIM®. McKusick-Nathans Institute of Genetic Medicine, Johns Hopkins University. Accessed 3 August 2023, https://omim.org/
31. Kang KW, Kim W, Cho YW, *et al.* Genetic characteristics of non-familial epilepsy. *PeerJ*. 2019;7:e8278.
32. Landrum MJ, Lee JM, Riley GR, *et al.* ClinVar: Public archive of relationships among sequence variation and human phenotype. *Nucleic Acids Res*. 2014;42(Database issue):D980-D985.
33. Richards S, Aziz N, Bale S, *et al.* Standards and guidelines for the interpretation of sequence variants: A joint consensus recommendation of the American College of Medical Genetics and Genomics and the Association for Molecular Pathology. *Genet Med*. 2015;17(5):405-424.
34. Tate JG, Bamford S, Jubb HC, *et al.* COSMIC: The catalogue of somatic mutations in cancer. *Nucleic Acids Res*. 2019;47(D1):D941-D947.
35. Ribierre T, Deleuze C, Bacq A, *et al.* Second-hit mosaic mutation in mTORC1 repressor DEPDC5 causes focal cortical dysplasia-associated epilepsy. *J Clin Invest*. 2018;128(6):2452-2458.
36. Bonduelle T, Hartlieb T, Baldassari S, *et al.* Frequent SLC35A2 brain mosaicism in mild malformation of cortical development with oligodendroglial hyperplasia in epilepsy (MOGHE). *Acta Neuropathol Commun*. 2021;9(1):3.
37. Kim JH, Park JH, Lee J, *et al.* Ultra-low level somatic mutations and structural variations in focal cortical dysplasia type II. *Ann Neurol*. 2023;93(6):1082-1093.
38. Lai D, Gade M, Yang E, *et al.* Somatic variants in diverse genes leads to a spectrum of focal cortical malformations. *Brain*. 2022;145(8):2704-2720.
39. Mascarenhas R, Merrikh D, Khanbabaei M, *et al.* Detecting somatic variants in purified brain DNA obtained from surgically implanted depth electrodes in epilepsy. *medRxiv*. [Preprint] doi:https://doi.org/10.1101/2024.07.08.24310005
40. Lu HC, Tan Q, Rousseaux MW, *et al.* Disruption of the ATXN1-CIC complex causes a spectrum of neurobehavioral phenotypes in mice and humans. *Nat Genet*. 2017;49(4):527-536.
41. Dhawan A, Baitamouni S, Liu D, *et al.* Exploring the neurological features of individuals with germline PTEN variants: A multicenter study. *Ann Clin Transl Neurol*. 2024;11(5):1301-1309.
42. Yehia L, Keel E, Eng C. The clinical spectrum of PTEN mutations. *Annu Rev Med*. 2020;71:103-116.
43. Lai A, Soucy A, El Achkar CM, *et al.* The ClinGen brain malformation variant curation expert panel: Rules for somatic variants in AKT3, MTOR, PIK3CA, and PIK3R2. *Genet Med*. 2022;24(11):2240-2248.
44. Kim J, Park SM, Koh HY, *et al.* Threshold of somatic mosaicism leading to brain dysfunction with focal epilepsy. *Brain*. 2024;147(9):2983-2990.
45. Xu Q, Uliel-Sibony S, Dunham C, *et al.* mTOR inhibitors as a new therapeutic strategy in treatment resistant epilepsy in hemimegalencephaly: A case report. *J Child Neurol*. 2019;34(3):132-138.